Supporting Information

Hierarchical Composite of GeO_2 Nanotubes/N-doped Carbon Microspheres with High-Rate and Super-Durable Performance for Lithium-Ion Batteries

Lijing Han, [a, b] Jing Tang, [b] Qiaohua Wei, [b]* Congrong Chen, [a] Mingdeng Wei [a, c]*

[a] Fujian Provincial Key Laboratory of Electrochemical Energy Storage Materials, Fuzhou University, Fujian 350116, China

[b] Ministry of Education Key Laboratory for Analytical Science of Food Safety and biology, Fujian Provincial Key Laboratory of Analysis and Detection Technology for Food Safety, Fuzhou University, Fuzhou, Fujian 350116, China

[c] Jiangsu Collaborative Innovation Center of Photovolatic Science and Engineering, Changzhou, 213164, China

[*] Corresponding authors. E-mail addresses: qhw76@fzu.edu.cn; wei-mingdeng@fzu.edu.cn

Experimental Section

Synthesis of GeO_2/NCS and GeO_2/NCT:

The 3D organic germanium precursors [$Ge(C_6H_4O_2)_2(bpy)$] was prepared according to a modified method in a previous report.[1] Typically, 5 mmol of GeO_2 and 10 mmol of catechol were are dispersed in 100 ml of deionized water, the mixture was placed in an oil bath at 105 ^oC for 2.5 h, When the temperature cooled down to 80 ^oC, 8 g of PVP and 5 mmol of 2,2-bipyridyl (bpy) were added under strong magnetic stirring, After 2 h, a yellow suspension was obtained by centrifugation, and then washed with deionized water and ethanol by several times, and drying under vacuum at 70 ^oC. The resulting organic germanium precursor was placed into a 30 ml crucible without a crucible lid in a muffler furnace and heated at 500 ^oC for 2 h with a rate of 5 ^oC min^{-1}.

As a control, GeO_2/NCT was fabricated in the same way as the GeO_2/NCS without adding PVP in the synthetic process.

Electrochemical test

The electrochemical properties of as-prepared samples were tested using 2025-type coin cells assembled in argon-filled glove box with oxygen and H_2O level below 0.1 ppm. Working electrodes were fabricated by mixing the active materials, carbon black, and polyvinylidene fluoride (PVDF) at a weight ratio of 8:1:1 in N-methylprrolidone (NMP). The obtained slurries were cast onto a copper current collector, and then dried overnight at 110 ^oC under vacuum. The mass loading of all electrodes was 0.7 mg/ cm^2. Electrochemical cells were assembled with the cast electrode, Li metal as both counter and reference electrodes, a microporous polypropylene membrane (Celgard 2400) was employed as the separator. The electrolyte was 1 M $LiPF_6$ in ethylene carbonate (EC), dimethyl carbonate (DMC), methyl ethyl carbonate (EMC) (1:1:1, by volume), and 6 wt% fluoride ethylene carbonate (FEC). All cells were cycled between 0.01 and 1.5 V versus Li/Li^+. Cyclic voltammetry (CV) and charge-discharge tests of all electrodes were performed using an electrochemical workstation (CHI 600 C) and Land automatic batteries tester (Land, CT 2001A, Wuhan, China), respectively.

Material characterization

TEM analysis was performed using a Scanning electron microscopy (SEM, Hitachi S4800 instrument) and transmission electron microscopy (TEM, Tecnai G2 F20 instrument FEI, USA) were applied for the determination of the morphology of samples. X-ray diffraction (XRD) patterns of samples were recorded on a Rigaku Ultima IV X-ray diffractomator by using Cu Kα radiation at a voltage of 40 KV and a current of 20 mA. FT-IR spectra were recorded on a BRUKER-EQUINOX-55 IR spectrophotometer and Raman spectra were conducted in a Renishaw in Via Raman microscope with a 532 nm laser. XPS spectra were analyzed use ESCALAB 250 confirm the chemical composition of samples. N_2 adsorption-desorption was performed on a Micromeritics ASAP 2020 instrument (Micromeritics, Norcross, GA, USA) at 77 K. Brunauer-Emmett-Teller (BET) and Barrett-Joyner-Halenda (BJH) analyses were used to calculate the specific surface area, and the corresponding pore size distribution. Thermogravimetric analysis (TGA) was characterized on CHNS/O analyzer (PE 2400II, Perkin-Elmer) by heating the samples in air up to 900 ^oC with a heating rate of 5 ^oC min^{-1} in order to determine the amount of germanium oxide residue in the powders.

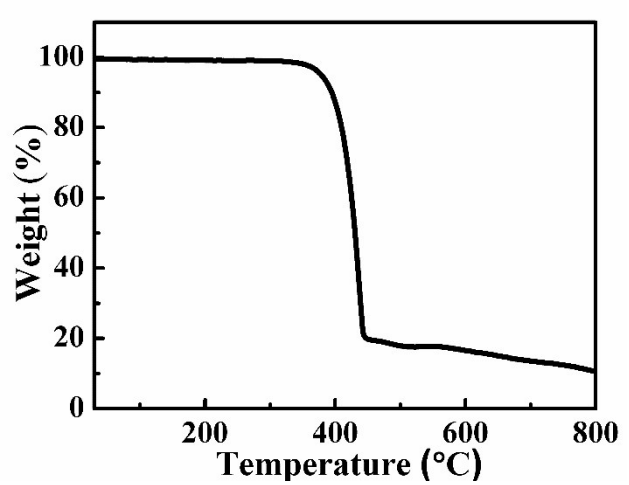

Fig. S1 TG curves of the 3D organic germanium complexes.

Fig. S1 shows the TGA curve of the precursor $Ge(C_6H_4O_2)_2(bpy)$. It shows one major stage of weight loss. Decomposition process is attributed to the loss of physically absorbed water and removal of the carbon or nitrogen on the form of CO, CO_2 and NO_2 gases, started at 343 °C and lasted up to 453 °C, resulting from the decomposition of the organic ligands. In addition, it loses smaller weight due to the reaction of the carbon with oxygen when the temperature beyond 453 °C. Hence, the thermal behavior of the precursors can be expressed by the following reactions:[2-4]

$Ge(C_6H_4O_2)_2(bpy) \rightarrow GeO_2/N\text{-}C + 8\ H_2O\uparrow + CO\uparrow + CO_2\uparrow + NO_2\uparrow$

$GeO_2/N\text{-}C + O_2 \rightarrow GeO_2 + CO_2\uparrow + NO_2\uparrow$

According to the above results, the calcination temperature was set at 500 °C, which can maintain a small amount of nitrogen-doped carbon to improve the stability and conductivity of the anode material.

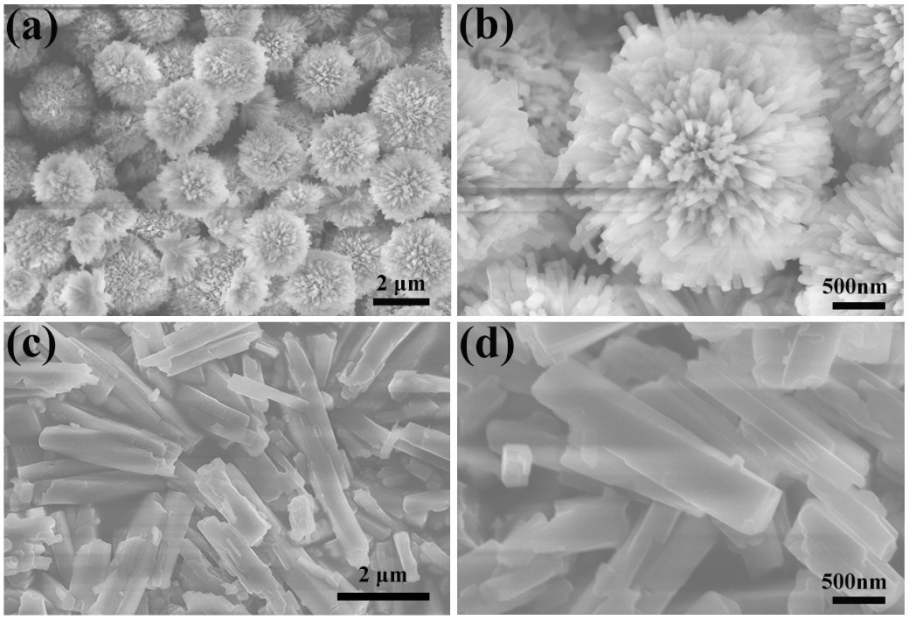

Fig. S2 SEM images of the organic germanium complexes: (a, b) 3D and (c, d) 1D.

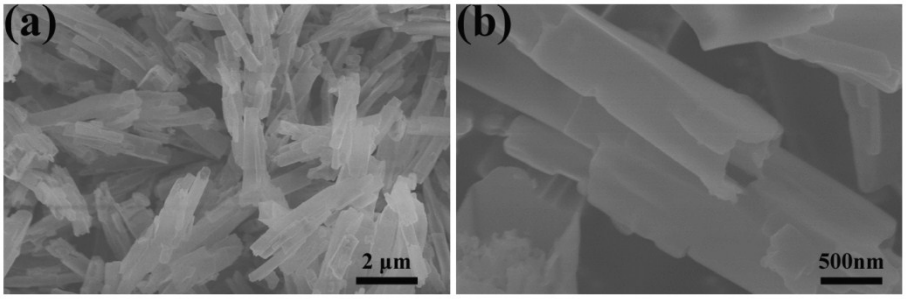

Fig. S3 (a, b) SEM images of the GeO_2/NCT.

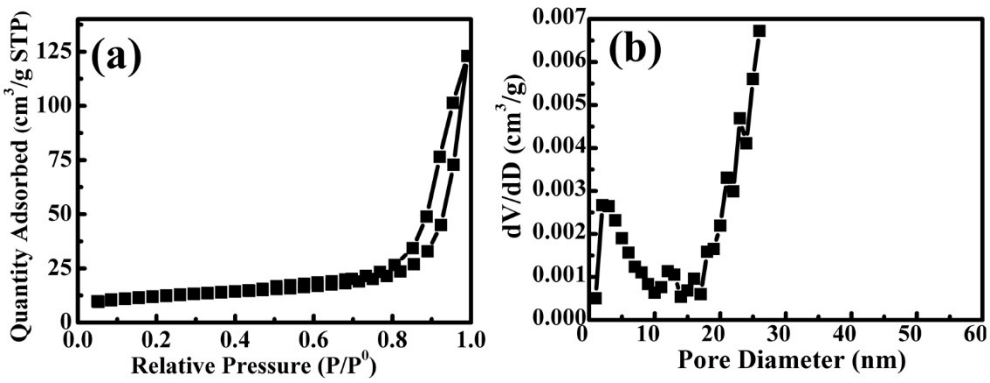

Fig. S4 (a) N_2 adsorption-desorption isotherms and (b) pore size distribution from the adsorption branch through the BJH method of GeO_2/NCS.

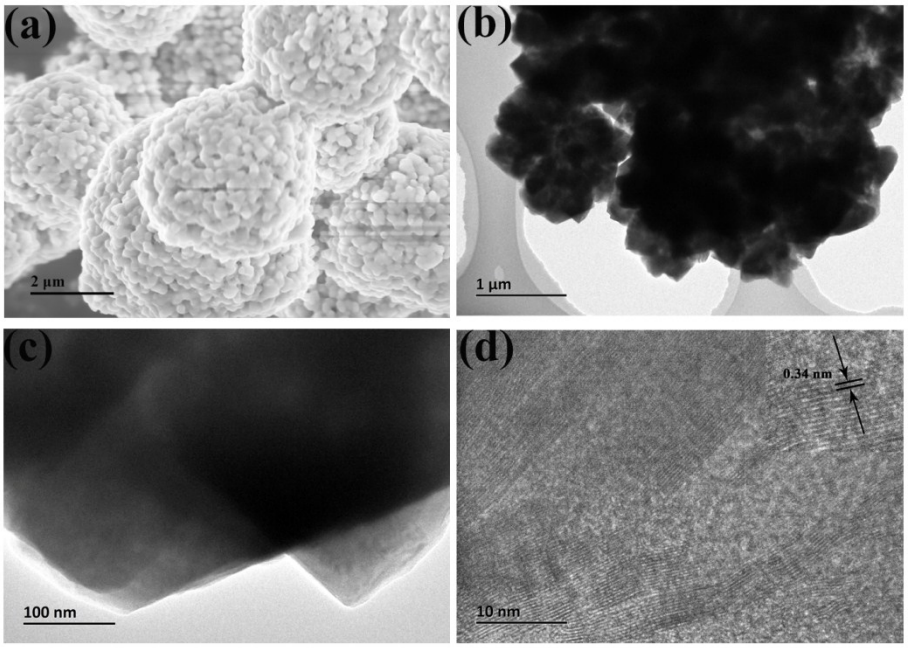

Fig. S5 (a) SEM image, (b-d) TEM images of GeO_2 calcined at 600 °C (inset: HRTEM image).

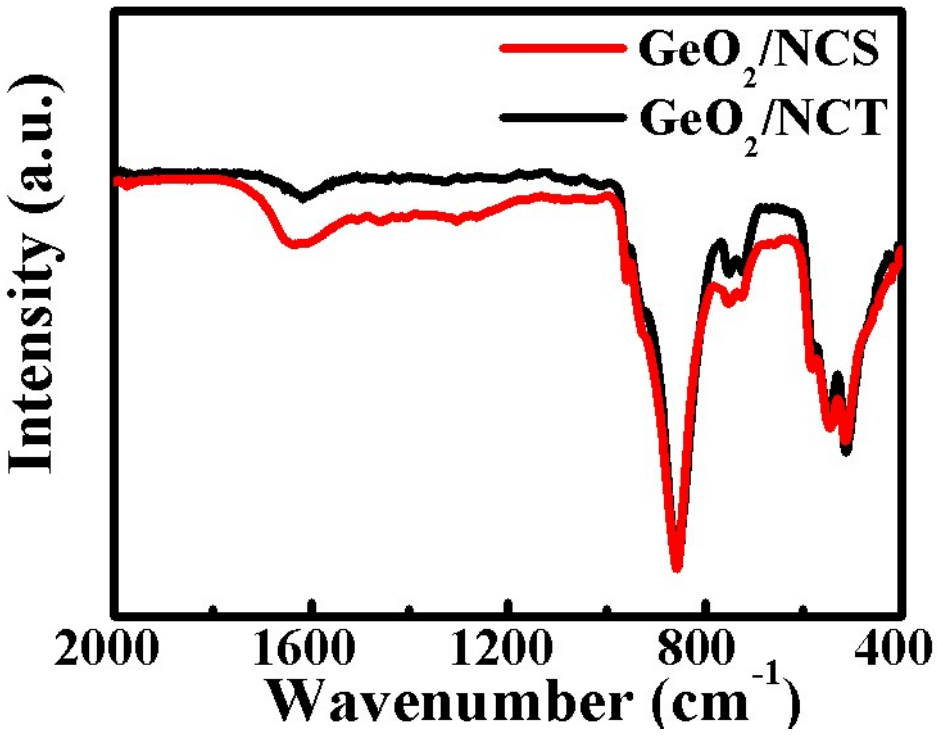

Fig. S6 FTIR sepctra of the GeO_2/NCS and GeO_2/NCT composites.

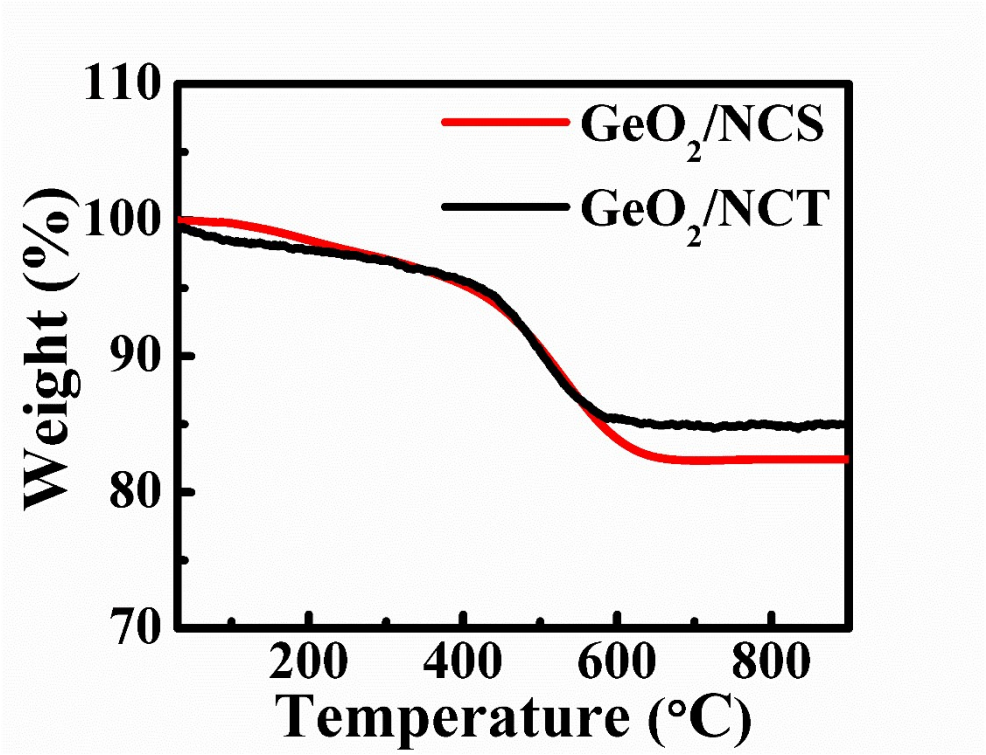

Fig. S7 TG curves of the GeO_2/NCS and GeO_2/NCT composites.

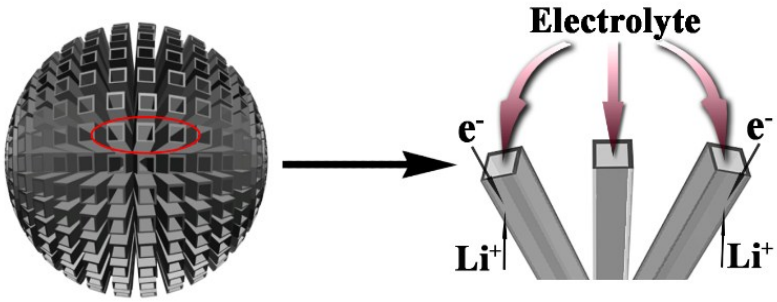

Fig. S8 Transport path of lithium ions and electrons in GeO_2/NCS composite.

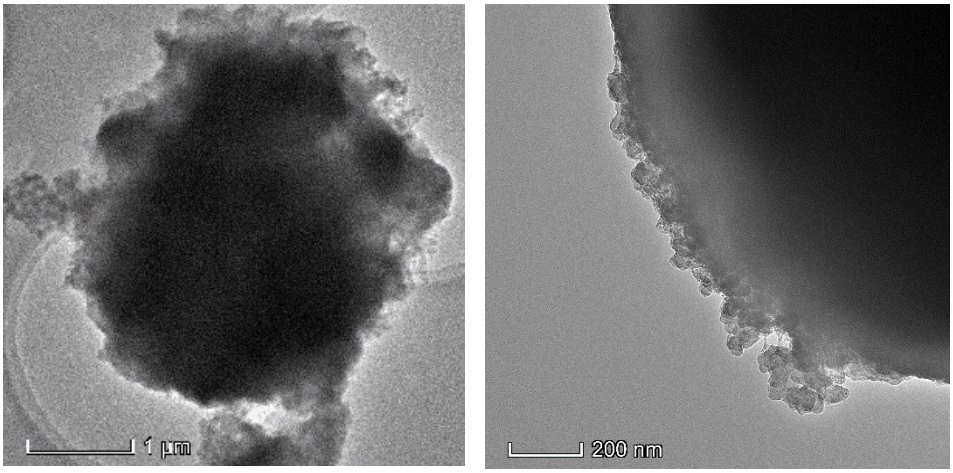

Fig. S9 The TEM images of GeO_2/NCS after 500 cycles at 1 A g^{-1}.

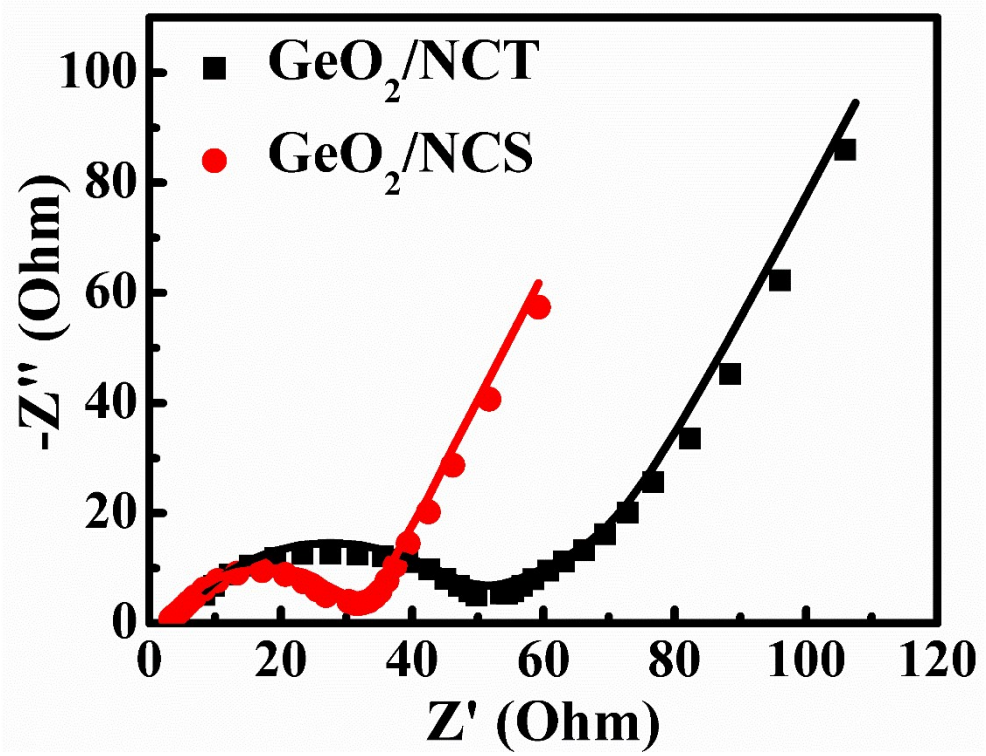

Fig. S10 Electrochemical impedance spectra of GeO_2/NCS and GeO_2/NCT after 100 cycles.

Table. S1 comparison of electrochemical properties of GeO_2 anodes.

Anode	Voltage range (V)	Cycle stability			Ref.
		Current Density (mA g^{-1})	After n^{th} cycle	Charge capacity (mAh g^{-1})	
GeO_2/NCS	0.01-1.5	200 1000	100 500	804 789	This work
GeO_2/Ge	0.01-1.5	500	100	665.3	*Adv. Funct. Mater.*, 2019, 1807946
GeO_2 IO	0.01-1.5	150	250	714	*Nano Energy*, 2018, **43**, 11-21.
Hexagonal GeO_2	0-1.5	200	50	747	*Nanoscale*, 2017, **9**, 3961
rGO/GeO_2/PANI	0.005-2.0	100	100	749	*J. Power Sources*, 2016, **306**, 791
Ge/GeO_2/C	0.005-2.0	200	50	915	*Electrochim. Acta*, 2016, **188**, 120
GeO_2/C-N	0.01-1.5	550	400	871	*J. Mater. Chem. A,* 2015, **3**, 21722
GeO_2/C	0.01-1.5	550	200	905	*Nanoscale*, 2015, **7**, 2552
CNT-GeO_2	0.005-1.5	200	500	813.7	*New J. Chem.*, 2015, **39**, 689
GeO_2	0.01-1.5	100	50	1340	*Chem. Commun.*, 2014, **50**, 13956
GeO_2/MC	0.01-1.5	1500	380	452	*J. Power Sources*, 2014, **269**, 755
GeO_2/C	0-1.5	110	50	697	*Electrochim. Acta*, 2014, **116**, 203
GeO_2	0.005-1.5	565 1130	100 500	816 574	*Nano Lett.*, 2014, **14**, 1005
GeO_2/G	0.01-1.5	110 2200	100 1000	919 571	*Adv. Energy Mate,* 2013, **3**, 1269

Notes and references

1 C. Jing, W. Li, L. Yang, Z. Shi, Q. Luo, *Chinese Journal of Inorganic Chemistry*, 1998, **14**, 261-265.
2 D. T. Ngo, R. S. Kalubarme, M. G. Chourashiya, C.-N. Park and C.-J. Park, *Electrochim. Acta*, 2014, **116**, 203-209.
3 W. Zhang, H. Pang, W. Sun, L.-P. Lv and Y. Wang, *Electrochem. Commun.*, 2017, **84**, 80-85.
4 J. Zhang, T. Yu, J. Chen, H. Liu, D. Su, Z. Tang, J. Xie, L. Chen, A. Yuan and Q. Kong, *Ceram. Int.*, 2018, **44**, 1127-1133.